



Characterization of CNPY5 and its family members

Danny Schildknecht,¹ Naomi Lodder,¹ Abhinav Pandey,¹ Maarten Egmond,² Florentina Pena,¹ Ineke Braakman ¹ and Peter van der Sluijs ^{1*}

¹Cellular Protein Chemistry, Bijvoet Center for Biomolecular Research, Utrecht University, Utrecht, The Netherlands

²Membrane Biochemistry and Biophysics, Bijvoet Center for Biomolecular Research, Utrecht University, Utrecht, The Netherlands

Received 29 March 2019; Accepted 29 April 2019

DOI: 10.1002/pro.3635

Published online 16 May 2019 proteinscience.org

Abstract: The Canopy (CNPY) family consists of four members predicted to be soluble proteins localized to the endoplasmic reticulum (ER). They are involved in a wide array of processes, including angiogenesis, cell adhesion, and host defense. CNPYs are thought to do so via regulation of secretory transport of a diverse group of proteins, such as immunoglobulin M, growth factor receptors, toll-like receptors, and the low-density lipoprotein receptor. Thus far, a comparative analysis of the mammalian CNPY family is missing. Bioinformatic analysis shows that mammalian CNPYs, except the CNPY1 homolog, have N-terminal signal sequences and C-terminal ER-retention signals and that mammals have an additional member CNPY5, also known as plasma cell-induced ER protein 1/marginal zone B cell-specific protein 1. Canopy proteins are particularly homologous in four hydrophobic alpha-helical regions and contain three conserved disulfide bonds. This sequence signature is characteristic for the saposin-like superfamily and strongly argues that CNPYs share this common saposin fold. We showed that CNPY2, 3, 4, and 5 (termed CNPYs) localize to the ER. In radioactive pulse-chase experiments, we found that CNPYs rapidly form disulfide bonds and fold within minutes into their native forms. Disulfide bonds in native CNPYs remain sensitive to low concentrations of dithiothreitol (DTT) suggesting that the cysteine residues forming them are relatively accessible to solutes. Possible roles of CNPYs in the folding of secretory proteins in the ER are discussed.

Keywords: Canopy (CNPY) proteins; ER; protein folding; MZB1; pERp1; CNPY5; B lymphocyte

Additional Supporting Information may be found in the online version of this article.

Grant sponsor: Innovatiegerichte Onderzoeksprogramma Genomics IGE07004B; Grant sponsor: Nederlandse Organisatie voor Wetenschappelijk Onderzoek 700.55.751 711.012.008 IGE07004; Grant sponsor: Seventh Framework Programme 235649; Grant sponsor: EUROCORES Programme EuroSCOPE of the European Science Foundation and Netherlands Science Organization; Grant sponsor: Marie-Curie Actions of the 7th Framework Programme of the EU Innovative Training Network "Virus Entry".

*Correspondence to: Peter van der Sluijs, Cellular Protein Chemistry, Bijvoet Center for Biomolecular Research, Utrecht University, Padualaan 8, 3584 CH, Utrecht, The Netherlands.

E-mail: p.vandersluijs1@uu.nl

This is an open access article under the terms of the Creative Commons Attribution-NonCommercial License, which permits use, distribution and reproduction in any medium, provided the original work is properly cited and is not used for commercial purposes.

Introduction

The Canopy (CNPY) family was originally defined by the discovery of CNPY1 in zebrafish. The name derives from the morphology of zebrafish embryos lacking CNPY1, which have the appearance of an airplane canopy.^{1,2} The five Canopy proteins belong to the saposin-like protein (SAPLIP) superfamily whose members include among others the four saposins, acid sphingomyelinase involved in CD1 lipid antigen presentation and lipid homeostasis, and antimicrobial effectors in cytotoxic lymphocytes such as NK-lysin.¹ Their defining features include six strictly conserved cysteines in a characteristic disulfide bond pattern.² CNPYs are small 21–30 kDa proteins that are widely distributed and have been implicated in diverse biological processes. We first review distribution and function and then zoom in on some of their properties (Table I).

Table I. Properties of CNPY Family Members

	CNPY1	CNPY2	CNPY3	CNPY4	CNPY5
Molecular data					
Alternative name	-	pERp2, MSAP	pERp3, PRAT4A	pERp4, PRAT4B	pERp1, Mzb1
Gene ID	285888	10330	10695	245812	51237
Chromosome, location	7q36.3	12q15	6p21.1	7q22.1	5q31.2
Protein (aa)	92	182	278	246	189
Mw (kDa)	108.29	185.42	274.67	256.74	184.38
Tissue distribution					
Liver, Gallbladder	-	M	M	M	A
Pancreas	-	M	M	M	A
GI tract	-	M	M	M	A
Skin	-	L	L	M	A
Kidney, urinary bladder	-	M	M	M	A
Male reproductive organs	-	M	M	M	A
Female reproductive organs	-	H	H	M	A
Muscle tissue	-	L	M	M	A
Immune system	-	L	H	M	M
Brain	-	M	H	M	A
Endocrine system	-	M	M	M	A
Respiratory system/lungs	-	M	L	M	A
Adipose, soft tissue	-	M	L	L	A
Functions					
	FGF signaling	LDLR metabolism	TLR1 and 4 surface trafficking	TLR1 and 4 surface trafficking	Immunoglobulin M assembly and secretion and Integrin-mediated cell adhesion
	Brain development (zebrafish)	Regulation of expression	Cochaperone Grp94 client specific		B-cell development
		Enhances neurite outgrowth			

CNPY1 has been studied mainly in the zebrafish in which it is an endoplasmic reticulum (ER) resident protein, specifically expressed in the midbrain-hindbrain boundary. A CNPY1 knockdown negatively influences maintenance, rather than development, of the midbrain-hindbrain boundary² and the dorsal forerunner cell clustering that precedes Kupffer's vesicle formation.³ Both these processes rely on fibroblast-growth-factor (FGF) signaling, and CNPY1 interacts with and promotes cell surface expression of the FGF receptor (FGFR). This suggests that CNPY1, as an ER-resident protein, may be involved in biosynthesis of FGFR. The observation that CNPY1 expression is increased by FGF8 indicates a positive feedback loop that promotes FGF signaling by increasing the capacity of the cell to synthesize higher levels of FGFR.² Remarkably, mammalian CNPY1 homologs do not have the six conserved cysteine signature nor the leader peptide sequence and are half the size of zebrafish CNPY1. This suggests that the first exons of CNPY1 may have been deleted in evolution, resulting in a smaller protein (not shown). Alternatively, as mammalian cDNAs encoding N-terminal sequences with limited homology to zebrafish CNPY1 have been described, it is possible that full length mammalian CNPY1 has not been cloned yet.

The human protein atlas finds CNPY2 protein in all tissues, with the highest expression in the liver, gallbladder, epididymis, placenta, and several regions of the brain.⁴ CNPY2 is the most widely studied CNPY protein and has many different functions attributed to it. CNPY2 has been proposed to interact with myosin regulatory light chain interacting protein through its predicted N-terminal signal sequence.⁵ Others showed, however, that CNPY2 is a secreted hormone-like protein.⁶ Overexpression of CNPY2 increases the number of neurites on neuronal cells, stimulates angiogenesis, promotes proliferation and migration of smooth muscle cells, and delays the development of heart failure in cardiomyopathy. CNPY2 knockdown decreases the number of neuronal cells with neurites and diminishes the cell-surface expression of the low-density lipoprotein receptor in response to FGF21.⁷ Lower expression of CNPY2 also activates the p53 pathway and impairs colorectal tumor growth.⁸ This is consistent with observations that CNPY2 expression provides a poor prognosis in several cancers including pancreatic neuroendocrine neoplasm,⁹ renal cancer,¹⁰ and colorectal cancer.¹¹

CNPY3 protein is widely expressed, with highest levels in neurons, the gastrointestinal (GI) tract, and other glandular epithelia. Biallelic CNPY3 variants have reduced expression of the protein and cause early onset epileptic encephalopathy,¹² a collective term for neurological disorders characterized by developmental impairments and seizures from early infancy. Expression of CNPY3 in lymphoblastoid cells of these patients is severely reduced, and knockout mice show spastic or dystonic features. Earlier work in CNPY3 knockout animals already uncovered a role for CNPY3 in

toll-like receptor (TLR)-dependent innate and adaptive immunity.^{13–15} CNPY3 also may have a broader function in signaling through an interaction with the tumor suppressor leucine-rich repeats and immunoglobulin-like domains 1, which serves as negative regulator of several receptor tyrosine kinases.¹⁶

Database queries with CNPY3 yielded the homologous protein CNPY4 with 38% identity and the typical cysteine signature.¹⁷ CNPY4 is ubiquitously expressed with high levels in the GI tract, testis, spleen and thymus. In accord with a role in immune cells, mRNA expression was particularly high in B-cell lines. CNPY3 and CNPY4 were first described as TLR4-interacting proteins, and named PRAT4A and PRAT4B, respectively.^{17,18} Since then they have been shown to be involved in the cell surface expression of various TLRs in different cell types. CNPY3 is required for the ER exit of TLR1, 2, 4, 5, and 9.^{13,19} It associates with the ER chaperone glucose-regulated protein 94 (Grp94, the ER paralog of cytoplasmic Hsp90) and with TLR4, and the interaction of both with TLR4 is required for its trafficking to the cell surface.¹⁴ This suggests that CNPY3 is needed for proper folding of TLR4 or for its release from ER chaperones. All TLRs for which CNPY3 is required are also clients of Grp94; therefore, CNPY3 has been suggested to be a TLR-specific cochaperone of Grp94.²⁰

CNPY4 also interacts with newly synthesized TLR4. Knockdown of CNPY4 decreased the surface expression of TLR4 when levels of CNPY3 remained the same, indicating that these proteins have nonredundant roles.¹⁷ In accord, CNPY3 and CNPY4 act antagonistically on the cell surface expression of TLR1: CNPY3 promotes trafficking while CNPY4 blocks it.²¹ Balance of the two is likely part of the regulation of TLR1 surface expression and may also extend to other TLRs.

Recent bioinformatic analysis showed that a small protein independently cloned as plasma cell-induced ER protein 1 (pERp1)^{22–25} or marginal zone B cell-specific protein 1 (MZB1)^{26,27} has the typical features of a bona fide CNPY protein and should be included as CNPY5 in the Canopy family.²⁸ CNPY5 is expressed mostly in the spleen and bone marrow^{16–18} and particularly in cells of the B lymphocyte lineage and in plasmacytoid dendritic cells.^{25,29} We identified CNPY5 as a protein that is upregulated as a consequence of lipopolysaccharide (LPS)-induced B-cell differentiation.²² During this process, B cells expand their ER and boost expression of many chaperones and other proteins that are required for proper folding of the vast number of immunoglobulins (and other proteins) that they secrete during a humoral immune response. Another clue to CNPY5 function emerged from studies of the Hendershot lab who characterized CNPY5 as member of a multiprotein complex in the ER that is associated with the Hsp70-type chaperone BiP.²⁴ This complex also contains several other ER chaperones assisting in oxidative folding such as Grp94 and ER protein 72.³⁰ Interestingly, CNPY2 and

CNPY3 have also been found in complexes with Grp94^{14,15,31} and BiP,³¹ suggesting a broader role for CNPYs in ER protein folding. Consistent with such a function are the phenotypes arising after reduced expression of CNPY5, which include folding and secretion defects of immunoglobulin M, and impaired integrin-mediated cell adhesion and pro- to pre-B-cell differentiation.^{24,25,27}

Thus far, members of the mammalian CNPY family have largely been investigated individually. We here studied the characteristics of CNPYs as a family with the aim of defining their location, folding, and role within the mammalian cell. We found that the CNPYs are a family of ER-resident proteins that form disulfide bonds, of which at least some remain sensitive to low concentrations of DTT, suggesting that the cysteine residues forming them are relatively accessible to solutes. Possible roles of CNPYs in the folding of secretory proteins in the ER are discussed.

Results and Discussion

Bioinformatic analysis of CNPY proteins

CNPY proteins range from 182 to 278 amino acids and share the signature six cysteines that form three intramolecular disulfide bonds in a very specific pattern, typical for members of the SAPLIP protein family.³² The two most N-terminal cysteines resemble the CXXC motif characteristic of thioredoxin-like oxidoreductase active sites [Fig. 1(A)].³³ The C-terminal cysteines in CNPY1 homolog, CNPY2, and CNPY5 form a conserved C(X)₆C motif, whereas CNPY3 and CNPY4 have an additional five residues between these two cysteines, making redox activity less likely. Indeed a direct evaluation of thiol reductase activity of CNPY5 by us and others showed little if any of such activity.^{24,25}

Clearly, the poor alignment and differences in predicted secondary structures between CNPYs indicate that each CNPY member is unique in the regions outside helices H1–H4 [Fig. 1(B)]. In particular, many residues interspaced between helices H2 and H3 are highly conserved in, for instance, CNPY3 and CNPY4, yet absent in CNPY2 and CNPY5. Of note is the unique sequence LxGPGL of CNPY5, which is not present in the other CNPYs. Remarkable differences are also present for the C-terminal regions immediately upstream of the ER-retention signals, as well as in the retention signals themselves. CNPY3 contains a stretch of positively charged (lysine) residues varying in length among the CNPY3 members, whereas CNPY4 contains a stretch of negatively charged (glutamate) residues, also varying in length. These large extensions are absent in both CNPY2 and CNPY5, suggesting that functional differences in CNPYs most likely arise from the residues shown in Figure 1(B).

Because the pattern of hydrophobic and hydrophilic residues in the conserved regions was strikingly similar

between CNPYs and saposins [Fig. 1(A)], we examined whether the helices in the CNPY family are also amphipathic, like in the saposin family members. Helical-wheel presentations are depicted (Fig. 2) for helices H1, H2, and H3 of saposins, based on the alignment shown in Figure 1(A). Helical wheels of saposin helices H1, H2, and H3 (inner wheel) aligned with those of CNPY5 and CNPY2 (outer two wheels) revealing that hydrophobic residues in saposin A (sapA), CNPY5, and CNPY2 match quite well, although the CNPY helices are slightly less amphipathic than those of sapA. Of note, the cysteine residues in H1 and H3 are located at the hydrophobic side of the helices.

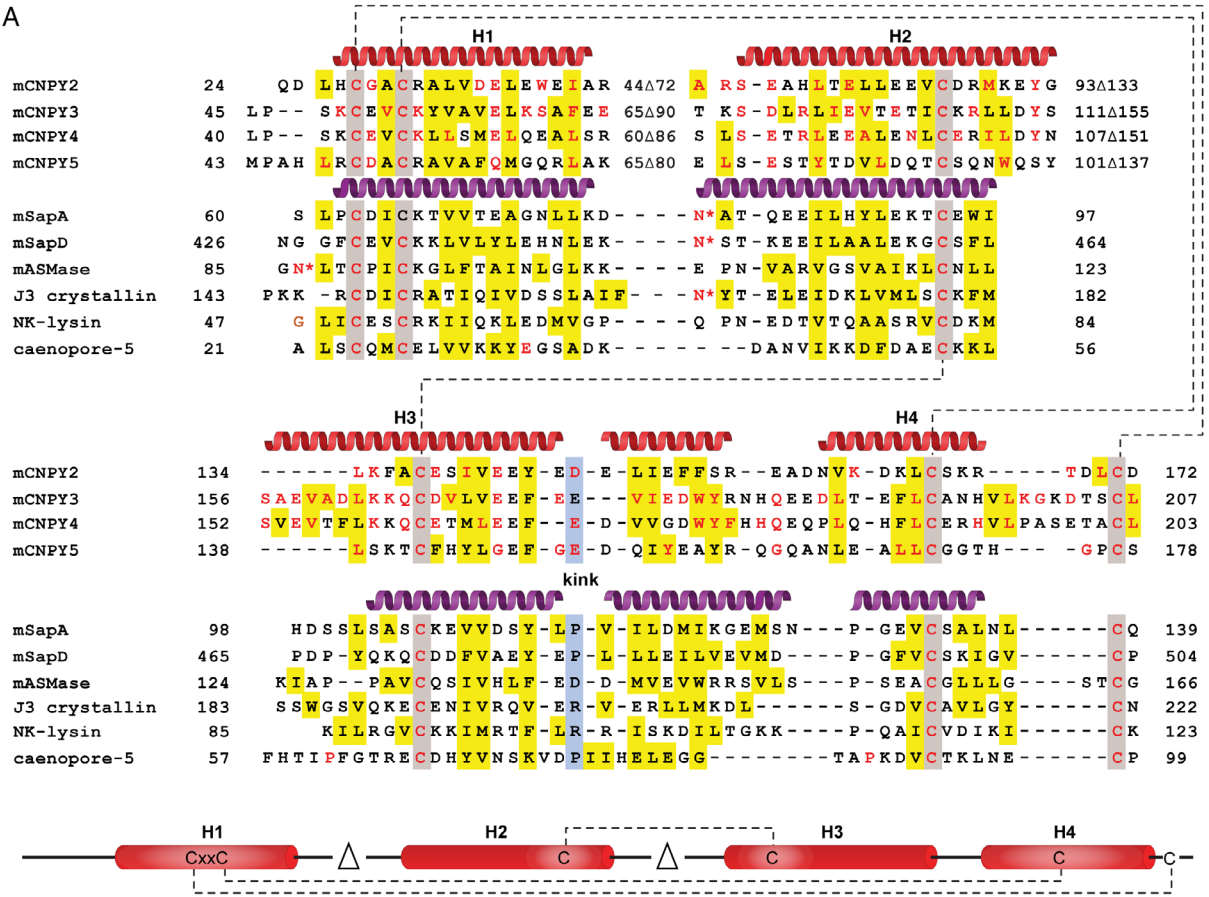
Although several structures have been published for SAPLIP proteins,³⁴ structural information of the Canopy family is lacking. Using the homology of the amphipathic helices, we checked whether existing structures reveal information for the Canopy family. SAPLIPS were first shown to be monomers such as the antimicrobial peptides NK lysin³² and caenopore-5,³⁵ both with membrane pore-forming properties. More recently, however, very different structures were obtained for two other SAPLIP-family members, galactocerebrosidase³⁶ and acid sphingomyelinase,³⁷ which show dimeric species. Through a conformational change between helices H1 and H2, these structures can open up, thereby exposing large hydrophobic surfaces. The two proteins form dimers in different ways that both involve packing of the exposed hydrophobic surfaces. Whereas the C and D chains of galactocerebrosidase pack in parallel fashion,³⁶ the two sphingomyelinase proteins pack in an antiparallel way.³⁷

Based on the highly conserved amphipathic helices and disulfide-bonding patterns, we propose that similar conformational changes occur in Canopy proteins leading to dimerization. This is supported by literature showing that CNPYs can occur as monomeric and dimeric species. It is unlikely that specific lipid species are bound to these dimeric species as found for the sphingolipid processing enzymes discussed above,^{36,37} although an interaction with membranes cannot be excluded.

Full-length CNPYs localize to the ER

CNPYs have N-terminal hydrophobic stretches with a high propensity to serve as signal sequences, as predicted by SignalP (Supporting Information Fig. S1). The algorithm we used to predict signal peptides is aimed to discriminate between a transmembrane domain and a signal peptide that is cleaved.³⁸ Indeed we previously showed experimentally that CNPY5 is cleaved at the predicted sites.²³ The software predicts cleavage for all CNPYs, indicating that these N-terminal stretches are cleaved signal peptides and not transmembrane domains. Mammalian CNPY1 homolog (but not zebrafish CNPY1) misses a signal sequence (Supporting Information Fig. S1) most likely because mammalian CNPY1 homolog is similar to only the C-terminal half of zebrafish CNPY1 and

A



B

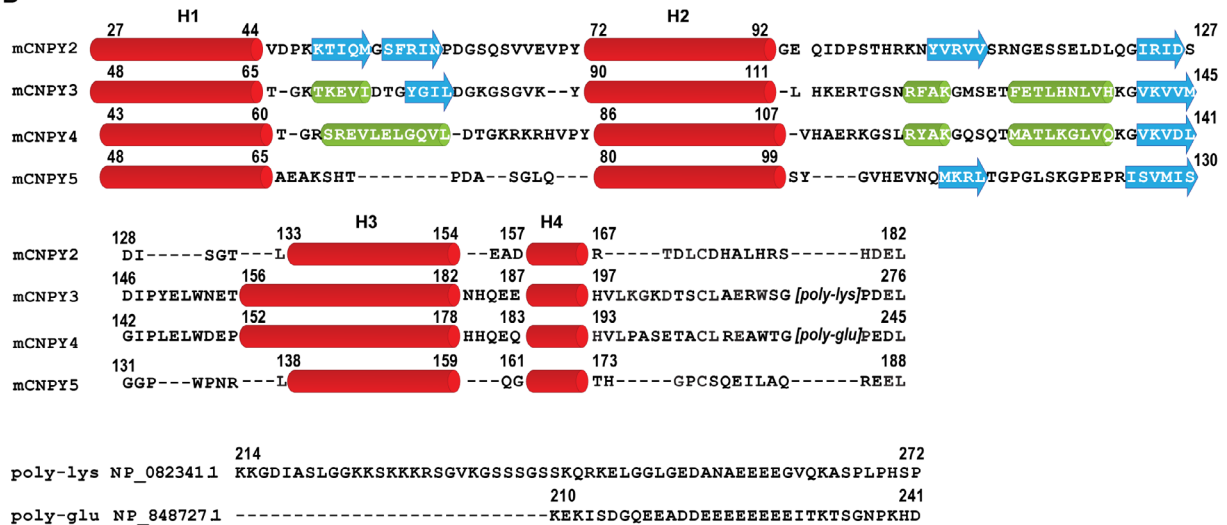


Figure 1. Alignment of CNPY and saposin-like proteins. (A) Amino-acid alignment of partial CNPY sequences and saposin-like proteins reveal structurally conserved helical regions (H1 to H4). The disulfide bonds connecting the cysteine residues are predicted to be conserved for all aligned proteins and are shaded gray. For CNPY2, these are cys28-cys171, cys31-cys164, and cys86-cys137 and for CNPY5 cys49-cys177, cys52-cys170, and cys94-cys142. Nonpolar hydrophobic or aromatic residues are shaded yellow, and highly (>95%) conserved residues are shown in red. The residues indicated with the blue shaded column in helix H3 correspond with the location of a kink in H3 as found, for example, in the structure of sapA. Δ indicates, for instance, that residues 93-133 in 93Δ133 are not shown in the alignment. (B) Sequence comparison of residues interspaced between the helical regions H1 and H4 shows unique sequences for CNPY family members. Red bars denote alpha helical structures H1 through H4 as in panel (A). Predicted alpha helices and beta strands are shown in green and blue, respectively, and conserved residues within each CNPY are shown in white. The region C-terminal to predicted H4 of CNPY3 is enriched in lysine residues as indicated with [poly-lys] while this part of CNPY4 is abundant with glutamic acid residues [poly-glu].

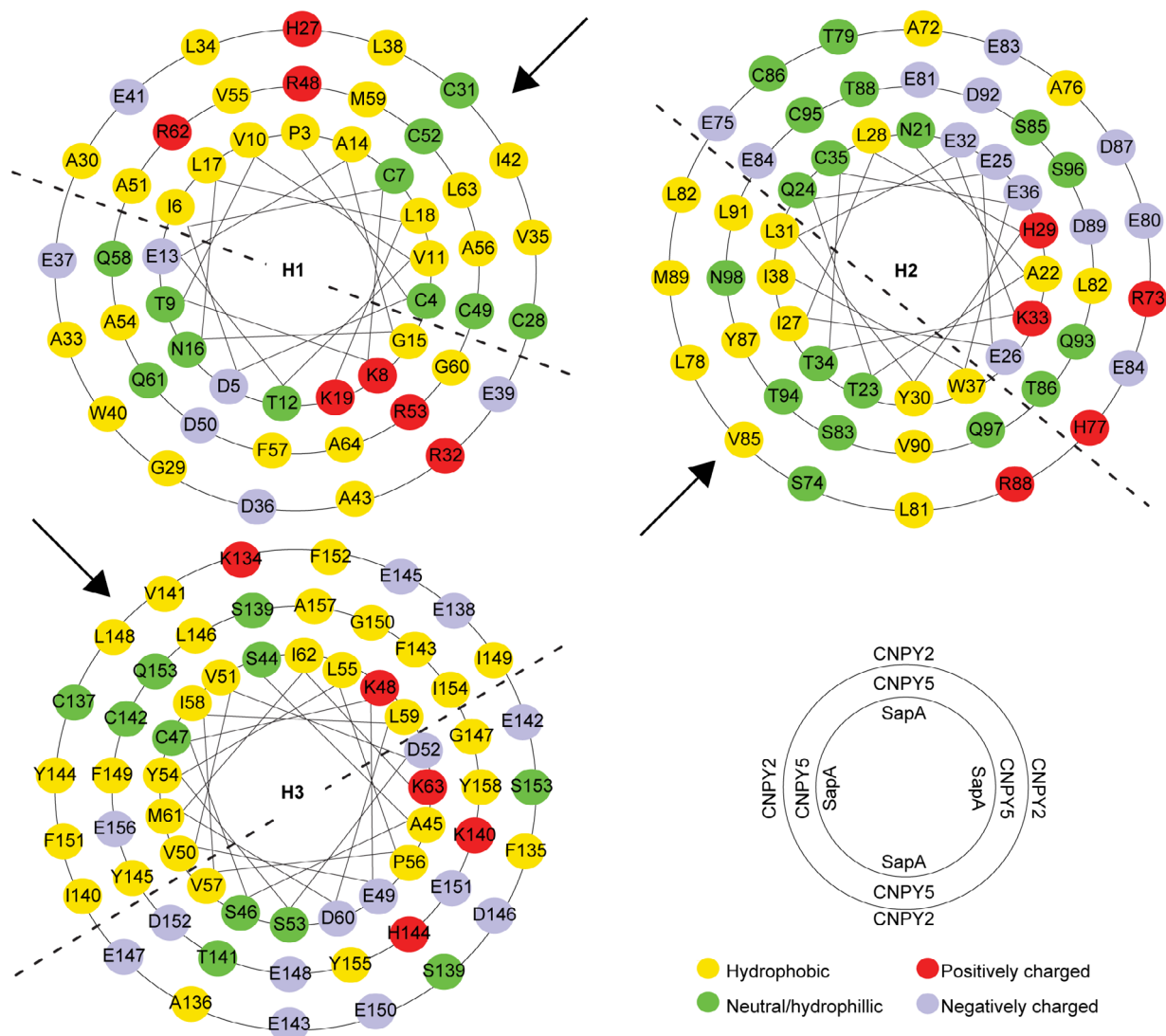


Figure 2. The hydrophobic surface of saposin-like proteins and dimerization. (A) Helical-wheel presentation of saposin helices H1, H2, and H3 (inner wheel) aligned with those of CNPY5 and CNPY2 (outer wheels). Color coding: Hydrophobic residues, yellow; neutral and hydrophilic, green; negatively charged, blue; and positively charged, red. The black arrow points to the most hydrophobic sides of the helices shown.

lacks the N-terminal half. CNPYs also contain C-terminal KDEL-type ER-retrieval signals HDEL (CNPY2), PDEL (CNPY3), PEDL (CNPY4), and REEL (CNPY5) [Fig. 1(B)]. Nevertheless, localization of CNPY proteins is incompletely understood, especially because the PDEL and PEDL sequences are poor retrieval signals^{39,40} and as CNPY2 also has been found extracellularly.⁶ We therefore evaluated the localization of CNPYs after transfection of HA-tagged constructs in HeLa cells. Control experiments revealed that the C-terminal HA tag does not interfere with the localization of CNPY5 (compare Fig. 3 and Supporting Information Fig. S4) and the other CNPYs (not shown) to the ER. Using double-label confocal immunofluorescence microscopy with antibodies against HA and PDI, we found that CNPY2, 3, 4, and 5 extensively colocalized with the ER marker (Fig. 3). Occasional colocalization was seen between CNPY4 (but not for the other CNPYs) with the cis Golgi marker

GM130 (Supporting Information Fig. S2). To address the localization of human CNPY1 homolog, we analyzed the distribution of GFP tagged human and zebrafish CNPY1 expressed in HeLa cells. Although zebrafish CNPY1 clearly localized to PDI-positive structures (Supporting Information Fig. S3), human CNPY1 homolog was diffusely present throughout the cytoplasm, in agreement with the absence of a predicted signal peptide. Taken together, bioinformatic analysis and immunofluorescence microscopy confirm that the full-length CNPYs are (predominately) resident ER proteins.

CNPYs form disulfide bonds with similar kinetics

We next analyzed disulfide bond formation between the cysteine residues in the CNPY proteins. We therefore performed radiolabeling pulse-chase experiments with ³⁵S-methionine/cysteine in HeLa cells expressing HA-tagged CNPY2, CNPY3, CNPY4, and CNPY5.

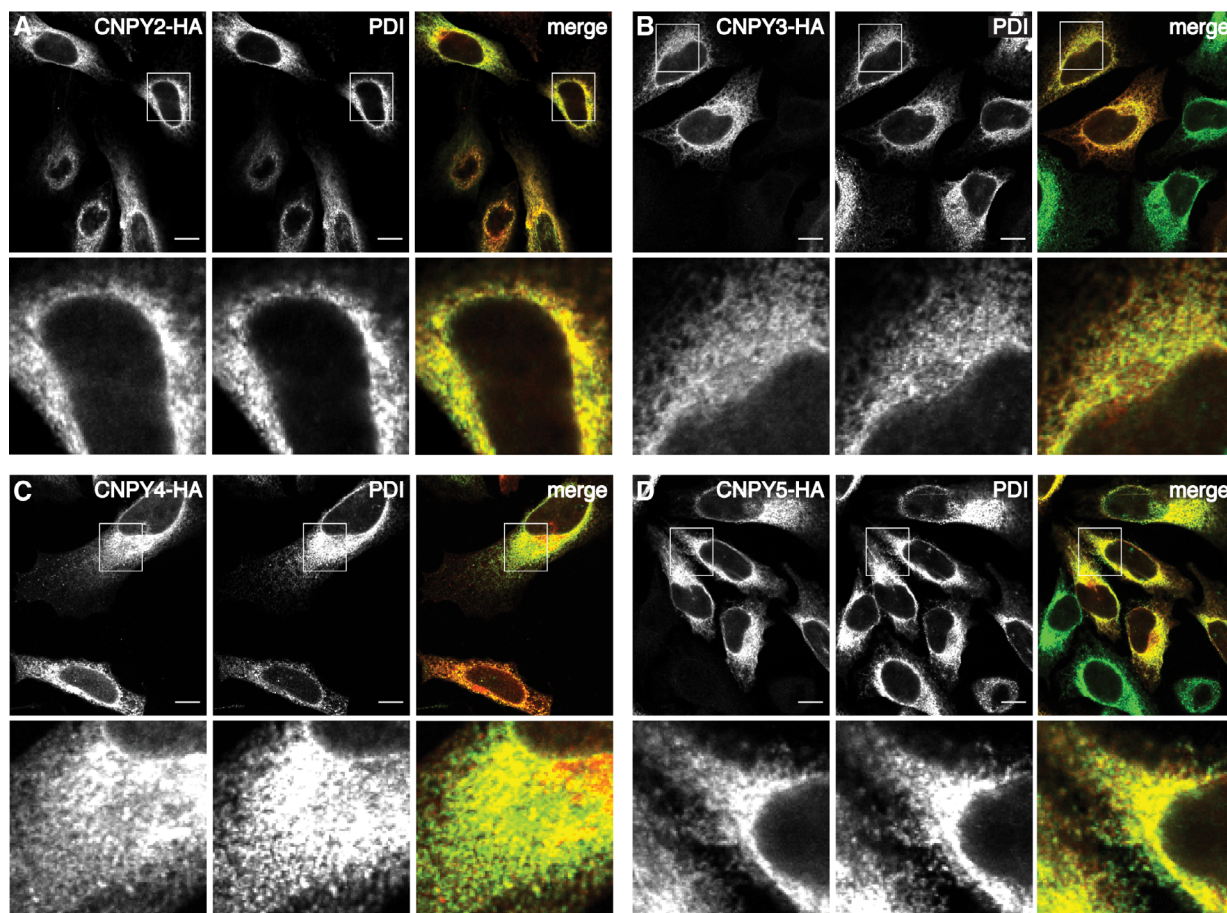


Figure 3. CNPY proteins are localized to the ER. Double-label confocal immunofluorescence microscopy of HeLa cells expressing HA-tagged CNPY labeled with rabbit antibodies against HA (red) and mouse against PDI (green). (A) CNPY2 versus PDI, (B) CNPY3 versus PDI, (C) CNPY4 versus PDI, and (D) CNPY5 versus PDI. Bar denotes 10 μ m.

Oxidative folding of the CNPYs was followed after synthesis under reducing conditions. Inclusion of 5 mM DTT during pulse labeling not only prevented cotranslational disulfide bond formation but also synchronized subsequent posttranslational folding in the absence of DTT [Fig. 4(A)]. In DTT, all CNPYs were synthesized as reduced species (R), which within 5 minutes of non-reducing chase started to form disulfide bonds and fold from R to the native conformation (NT) as shown on non-reducing sodium dodecyl sulfate-polyacrylamide electrophoresis (SDS-PAA) gels [Fig. 4(B), nonreducing panels]. All CNPYs formed not only some NT but also dimers and aggregates that poorly entered the nonreducing SDS-PAA gels. As most of those could be reverted upon reduction of the samples, part of the aggregates must have been linked by disulfides [Fig. 4(B), reducing panels]. As even in reducing SDS-PAGE some of the CNPYs were present in high-molecular-weight aggregates and stable, incompletely reduced monomers, we concluded that the CNPYs suffer from significant misfolding and aggregation under these conditions. Although we have not interrogated the individual disulfide bonds in each CNPY separately, their similar electrophoretic behaviors in Figure 4(B) suggest that they share their disulfide bond pattern with CNPY5²⁵ and other SACLIP proteins.

The native conformation of CNPYs has DTT-sensitive disulfide bonds

All CNPY proteins have an N-terminal copy of the CXXC motif typical for oxidoreductases catalyzing thiol-disulfide exchange reactions.⁴¹ We found CNPY5 to display weak oxidoreductase activity *in vitro*.²⁵ To perform their catalytic function, these disulfide bonds must be solvent accessible in the fully folded protein, as shown for PDI and Ero1, for instance,^{42–44} and therefore sensitive to reduction by agents like DTT. In contrast, structural disulfides are often not reducible in native, folded proteins.⁴⁵ To explore functionality of the disulfide bonds in CNPY proteins, we expressed HA-tagged CNPYs in HeLa cells and labeled the cells for 5 minutes with ³⁵S-methionine/cysteine. After a chase of 60 minutes, when CNPYs should be fully folded, the cells were incubated with DTT for 10 minutes, lysed, and CNPYs were immunoprecipitated with antibodies against HA [Fig. 5(A,B)].

CNPY2 was relatively resistant to DTT, as the addition of DTT during the last 10 minutes of the chase period did not affect the pool of native molecules nor aggregates, with only a minor fraction of reduced molecules generated by this treatment [Fig. 5(B)]. The other CNPYs were more sensitive to DTT treatment, as the band representing the

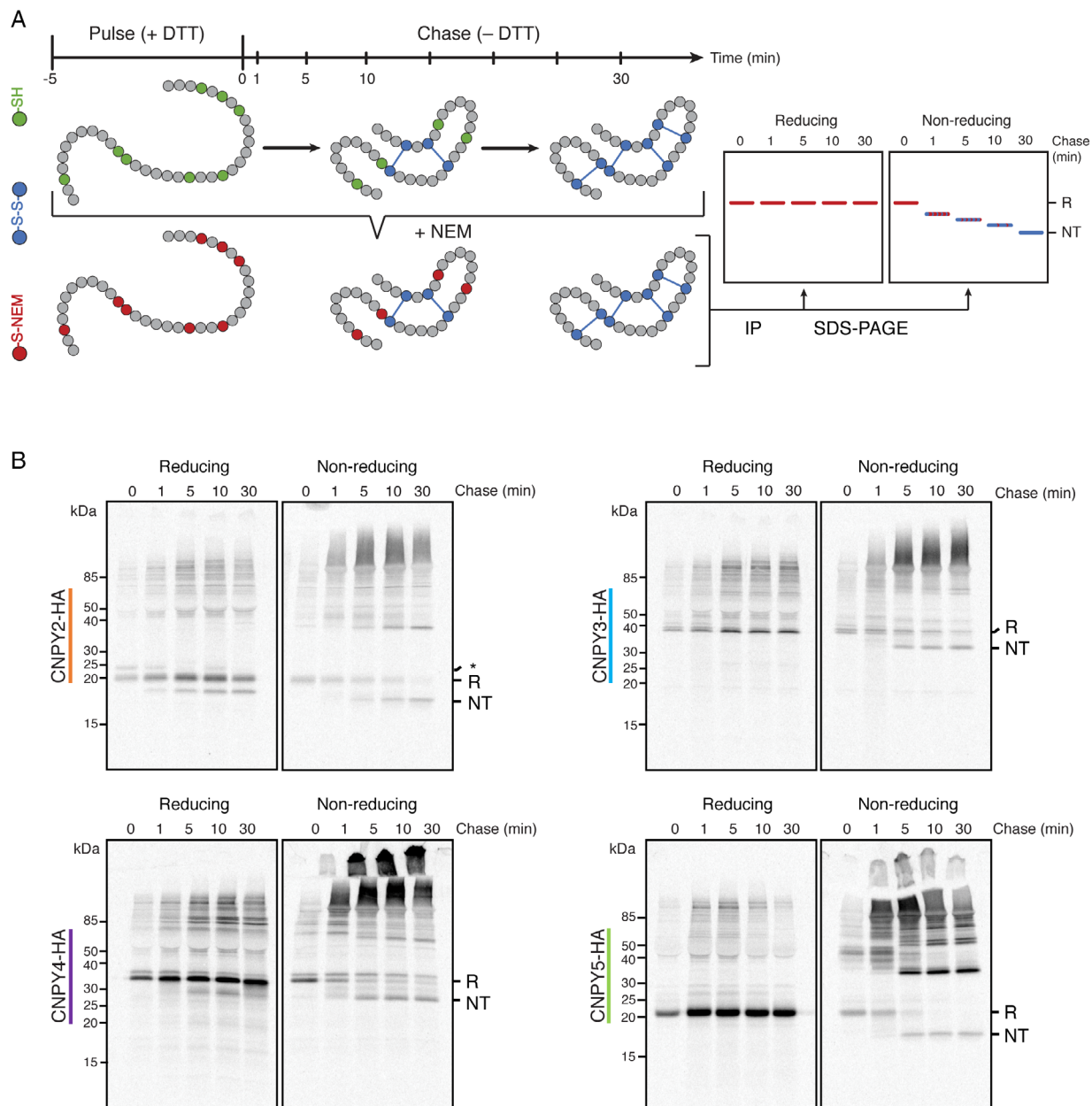


Figure 4. Oxidative folding of CNPY proteins. (A) Work flow of the experiment, with example gel. (B) HeLa cells were transfected with cDNAs encoding HA-tagged CNPY2, CNPY3, CNPY4, or CNPY5. The next day, cells were pulse labeled with ^{35}S -methionine/cysteine in the presence of 5 mM DTT. After 5 minutes, medium was aspirated and cells were chased for the indicated times without DTT, and subsequently lysed. CNPY proteins were immunoprecipitated with polyclonal antibody against HA. Samples were resolved by SDS-PAGE on nonreducing and reducing 15% gels. * denotes background band.

folded form largely shifted to a higher position in the gel, corresponding to the fully reduced conformation (CNPY3 and CNPY5) or intermediate forms (CNPY4 and CNPY5). These data show that not all disulfide bonds in CNPY proteins are buried, which suggests that some may be functional. A more rigorous assessment of their enzymatic properties, however, is needed to establish definitively whether there are functional differences between the CNPYs.

CNPY expression during B-cell activation

ER-resident proteins involved in biosynthesis, folding, or degradation of secretory proteins are usually upregulated

during ER stress through an unfolded protein response (UPR). The UPR is a response to the stress of overloading the ER with proteins that need to be folded.⁴⁶ Physiological examples of this include pancreatic β cells, which synthesize, fold, and secrete huge amounts of insulin,⁴⁷ or thyroglobulin-secreting thyrocytes.⁴⁸ We showed before that CNPY5 and ER chaperones are concomitantly upregulated during LPS-induced B-cell differentiation, a process in which the ER greatly expands to secrete antibodies for a humoral immune response and the UPR is activated.^{22,23,25} Conversely, as CNPY3 and CNPY4 are involved in the regulation of many cell surface TLRs and TLR responses,^{13,19} it is imperative

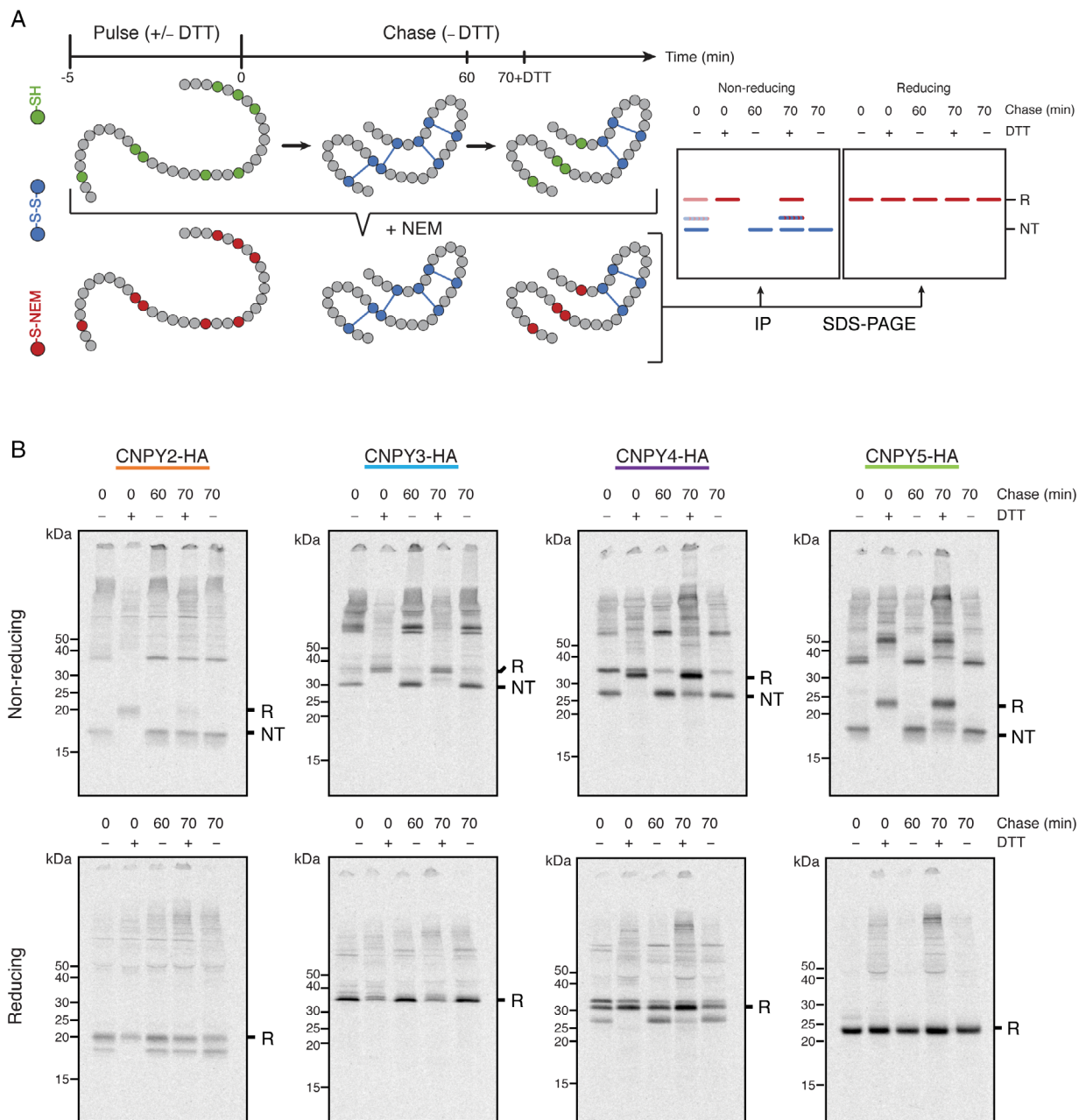


Figure 5. Native CNPY proteins have DTT-sensitive disulfide bonds. (A) Work flow of the experiment, with example gel. (B) HeLa cells overexpressing CNPYs 2–5 were pulse labeled with ^{35}S -methionine/cysteine for 5 minutes, then chased for 0, 60, or 70 minutes. The final 10 minutes of the 70 were in the absence or presence of 5 mM DTT, as indicated. CNPY proteins were immunoprecipitated via a C-terminal HA tag. Samples were analyzed by reducing and nonreducing SDS-PAGE as in Figure 4.

to understand whether CNPY expression in general is regulated during B cell differentiation. We therefore treated $\text{I.29}\mu^+$ cells for up to 4 days with LPS and first analyzed XBP1 splicing as readout for the UPR [Fig. 6 (A)]. It is clear from Figure 6(A) that the UPR is activated by LPS as XBP1 was progressively spliced during the first 3 days. We also verified by immune fluorescence microscopy that CNPY5 expression in the ER is increased [Fig. 6(B) and Supporting Information Fig. S4].^{22,23,25} To assess whether the other family members are regulated during this response, we studied their expression by

quantitative polymerase chain reaction (qPCR) [Fig. 6(C)] and Western blot [Fig. 6(D,E)]. CNPY5 mRNA and protein increased during activation and reached peak values on Days 3 and 4, respectively. CNPY5 is a relatively stable protein [Figs. 4(B) and 5(B)]; for this reason, CNPY5 protein expression decreases later than its mRNA levels likely when the $\text{I.29}\mu^+$ cells enter apoptosis. CNPY2 mRNA also increased upon activation, although not to the extent of CNPY5 mRNA, whereas the mRNAs of CNPY3 and CNPY4 were minimally altered. This suggests that the CNPYs have different roles in activated B cells.

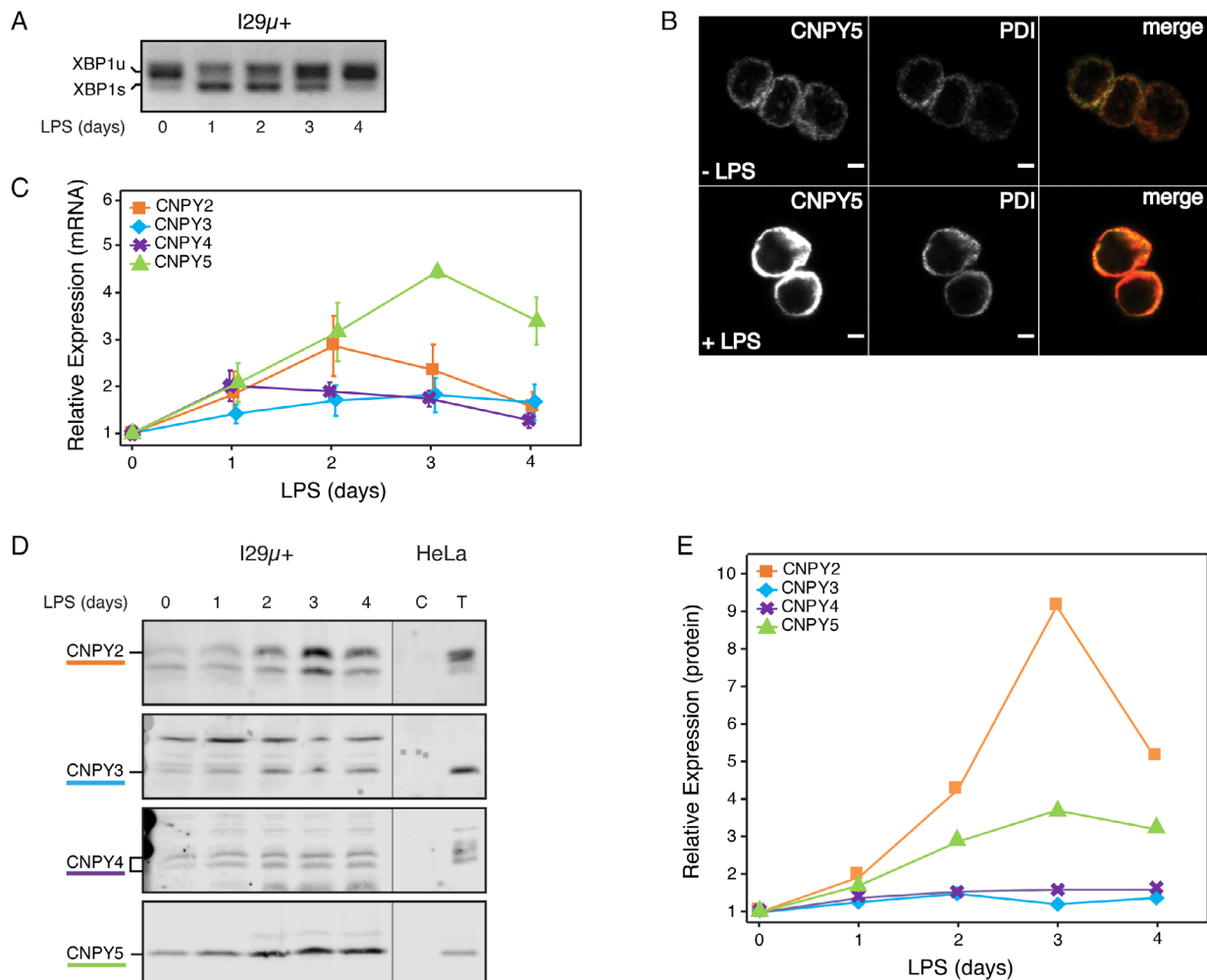


Figure 6. CNPY expression in differentiating I.29 μ^+ B cells. Mouse I.29 μ^+ cells were treated for up to 4 days with LPS. After different periods of time, cells were processed for (A) XBP1 splicing as assessed by RT-PCR, (B) localization of CNPY5 (red) using double label confocal immunofluorescence microscopy with PDI (green) as ER marker and evaluation of CNPY protein expression levels by (C) qPCR and (D, E) Western blot. XBP1u and XBP1s denote unspliced and spliced XBP1, respectively. Scale bar is 10 μ m.

Mode of action

The sequence homology of the CNPY proteins with saposins and the structural reorientation of the amphipathic helices noted in dimer formation for saposins may provide the first insight in the mode of action of CNPY proteins. The observed conformational change exposes a hydrophobic surface that facilitates interactions with partners. In SAPLIPs with antibacterial function such as NK lysin and caenopore-5, this surface is involved in interaction with lipids for generating a pore in bacterial membranes. For CNPY proteins, the exposure of a hydrophobic surface may lead to formation of both homo- and hetero-dimers. In addition, the exposed hydrophobic surface may help to prevent aggregation of incorrectly folded proteins. In contrast to saposins, CNPY proteins contain a large number of residues interspaced between the helices, many of which are highly conserved within a particular CNPY. These additional structures, particularly between helices H2 and H3, are not likely to interfere with the packing of helices H1 and H4. Structural integrity is controlled by the disulfide bond formed by the Cys

residue at the C-terminal end of H2 and the N-terminal Cys of H3 as well as by two disulfide bonds formed between the two N-terminal residues with the CXXC motif in H1 and the two C-terminal Cys residues [Fig. 1(A)]. When residues in between H2 and H3 interact specifically with other proteins, then CNPYs may help in dimerization of—or interaction between—two other proteins through CNPY dimer formation.

The homology of the Cys residues in CNPYs with SAPLIP proteins favors a structural role of the Cys residues in the CXXC motif and argues against a functional role of these Cys residues. In the thioredoxin family, free Cys SH groups are present, and the active site Cys residues in the CXXC motif are linked to each other.⁴¹ Neither of these features is shared with CNPYs. The comparison of CNPYs with SAPLIP proteins indicates that most Cys residues are close to hydrophobic residues and may therefore be shielded from solvent. We found, however, that CNPYs are sensitive to DTT to various extents. This again points to the large differences noted for CNPYs outside of the amphipathic helical regions. It

also leaves the option of oxidoreductase enzymatic activity we detect above background activity for CNPY5,²⁵ and which could be unleashed by reduction of regulatory disulfide bonds, as in Ero1.⁴⁹

The diverse functions of the CNPYs may be explained through a role in the folding of secretory proteins, perhaps as cochaperones of Grp94. Like CNPY3, CNPY5 interacts with a client of Grp94: immunoglobulin μ heavy chain,^{24,25,27} although an interaction of CNPY5 with Grp94 has not been shown under physiological conditions, other than in a multichaperone complex.²⁴ CNPY2 is involved in the trafficking of the LDL receptor,⁵⁰ another Grp94 client, and CNPY4 interacts with some TLRs, including TLR4 and TLR1. This suggests that the CNPY family members are good candidates for cochaperones of Grp94, and both CNPY2 and CNPY4 have been found to interact with Grp94.³¹ Each of the CNPYs has a different client protein or a different effect on client proteins, and thereby could confer client specificity to Grp94 or an extra layer of regulation in the case of CNPY3 and CNPY4, which act antagonistically on the cell surface expression of TLR1.^{14,21} In *Drosophila*, CNPY family member CNPYb, shown to be most similar to CNPY3, is a cochaperone for the *Drosophila* Grp94 homolog, gp93. Like CNPY3, it is also involved in TLR folding, indicating a conservation of CNPY3 action and of the cochaperone activity of the CNPY family.¹⁵

In summary, we have shown that pERp1/MZB1, now renamed CNPY5, belongs in the Canopy family. These proteins are small, ER-resident SAPLIPs with six conserved cysteines and a blocked CXXC motif. The CNPYs all oxidize, meaning that at least some of their conserved cysteines form disulfide bonds. If all cysteines form disulfide bonds then the pattern is likely to be the same as in CNPY5,²⁵ saposins, and other SAPLIPs. The diverse processes that the CNPYs have been shown to take part in point to functions as client-specific (co)chaperones in the ER, possibly working to help Grp94 fold a diverse set of client proteins.

Materials and Methods

Cells

HeLa cells were maintained in minimum essential medium (MEM) supplemented with 10% fetal bovine serum (FBS), nonessential amino acids and 2 mM Glutamax. I.29 μ^+ B cells were maintained in RPMI 1640 medium supplemented with 10% heat inactivated FBS, 1 mM sodium pyruvate, 2 mM Glutamax, and 50 μ M 2-mercaptoethanol. I.29 μ^+ B cells were activated with 20 μ g/mL LPS cells for up to 4 days. All cells were grown at 37°C with 5% CO₂.

DNA constructs and transfections

cDNAs encoding human CNPY2, mouse CNPY3, CNPY4, and CNPY5 were obtained from Research Genetics (Inchinnan, U.K.). CNPY2 and CNPY3 were ligated between the NdeI and NotI sites of pET28a. CNPY cDNAs

were ligated between KpnI and XhoI sites of pcDNA3. HA-tagged CNPY cDNAs were generated from CNPY pcDNA3.1 by PCR using the primers: 5'-TTGGGGACAA GTTTGTACAAAAAGCAGGCTGGTACCGCTACAAC AAGGCAAGGCTTG-3' (forward cmv primer) in combination with reverse primers 5'-TTGGGGTTGGGGA CCACTTTGTACAAGAAAGCTGGGTCTCGAGTCAT AGCTCATCATGAGCGTAATCTGGAACATCGTAT GGGTACGATATGTGCAGGGCATGGTC-3' (CNPY2), 5'-TTGGGGTTGGGGACCCTTTGTACAAGAAAGCT GGGTCTCGAGTCACAGCTCATCAGGAGCGTAATC TGGAACATCGTATGGGTAGGGGCTGTGTGGGA GGGGCG-3' (CNPY3) and 5'-TTGGGGTTGGGGACC ACTTTGTACAAGAAAGCTGGGTCTCGAGCTAAAG CTCTTCTCTAGCGTAATCTGGAACATCGTATGGG TACTGGGCCAGGATCTCCTGTG-3' (CNPY5). HA-CNPY4 was generated using 5'-GGGAATTCATGTGTGGA CTGCGTTTTT-3' (forward) and 5'-TGCTGCGCCGCTC AAAGATCTTCTGGTGCCTAGTCTGGTACGTCGTAT GGGTAGTCATGCTTGGGA-3' (reverse). This resulted in an HA tag directly in front of the last four amino acids, which allowed detection of all CNPYs with the same antibody. In control experiments, we established that the HA tag did not interfere with localization and function of the proteins (not shown). Human and codon optimized zebrafish CNPY1 cDNAs were generated from NM_001103176.1 (*hCNPY1* homolog) and NM_001039497.2 (*zfCNPY1*) sequences obtained from the NCBI database and cloned into pEGFP-N1 through Gibson assembly. For microscopy experiments, we transfected expression constructs using Lipofectamine 3000 (Thermo Fisher), whereas cells for pulse chase experiments were transfected using polyethylenimine (PEI) at a 2.5:1 PEI:DNA ratio. Transfected cells were washed with Hank's balanced salt solution after 24 hours and subsequently used in experiments.

Antibodies

His₆-tagged CNPY2 and CNPY3 expression was induced for 24 hours at 18°C. Recombinant proteins were affinity purified on Ni²⁺ NTA agarose according to standard protocols and used for immunization of rabbits. Antibodies against HA were generated by immunizing rabbits with a mixture of the two KLH-linked peptides YYDVPDYA YPYDVPDYAC and CYPYDVPDYAYPYDVPDYA. The rabbit antibody against CNPY5 has been described.²⁵ Affinity purified antibody against CNPY4 was from Sigma, the mouse monoclonal antibody ID3 against PDI has been described.⁵¹ The mouse monoclonal antibody against GM130 was from BD Biosciences, and fluorescently labeled secondary antibodies were purchased from Thermo Scientific.

Immunofluorescence microscopy

LPS-activated B cells and HeLa cells expressing tagged CNPY constructs were fixed with 2% paraformaldehyde (PFA) and permeabilized with 0.1% Triton X-100. HA-tagged CNPY proteins were double labeled with

rabbit anti HA and mouse ID3 antibodies, whereas B cells were labeled with rabbit anti CNPY5 and ID3. After washing with PBS/0.5% bovine serum albumin (BSA), cells were incubated with goat anti-rabbit Alexa488 and goat anti-mouse Alexa568 (Thermo Fisher). Cells were mounted with Prolong GOLD and imaged on a Zeiss LSM 700 confocal microscope. Images were processed with Image J and Photoshop.

Radioactive pulse-chase assays and immunoprecipitation

Radioactive pulse-chase and immunoprecipitation were performed as described previously.⁵² Briefly, cells were incubated for 15 minutes in MEM without methionine and cysteine (Thermo Fisher) and then labeled for 5 minutes with 66 μCi ³⁵S-methionine/cysteine (Perkin Elmer) per 35 mm dish. For some experiments, we included 5 mM DTT during labeling. After the pulse, cells were incubated at 37°C in MEM containing 5% FBS, 5 mM cysteine, 5 mM methionine, 2 mM Glutamax, and nonessential amino acids (chase medium) for the indicated times. At the end of the chase, dishes were transferred onto ice and washed with ice-cold HBSS containing 20 mM N-ethylmaleimide (NEM). Cells were lysed in 20 mM MES, 30 mM Tris-HCl pH 7.5, 100 mM NaCl with 0.5% Triton X-100, and 20 mM NEM, 1 mM phenylmethylsulfonyl fluoride (PMSF), and 10 $\mu\text{g}/\text{mL}$ of chymostatin, leupeptin, antipain, and pepstatin (CLAP). CNPY proteins were immunoprecipitated from detergent lysates with either HA or specific CNPY antibodies and Protein A-Sepharose beads. Immunoprecipitates were washed with 300 mM NaCl, 10 mM Tris-HCl pH 8.6, 0.05% SDS, and 0.05% Triton X-100. Beads were resuspended in 10 mM Tris-HCl pH 8.0 and 1 mM ethylenediaminetetraacetic acid (EDTA), pH 8.0, and immunoprecipitates were eluted with Laemmli sample buffer (200 mM Tris-HCl pH 6.8, 3% SDS, 10% glycerol, 1 mM EDTA, and 0.004% bromophenol blue, final concentrations) for 5 minutes at 95°C. Beads were centrifuged at 16,000g for 1 min and for the reducing samples 25 mM DTT was added to the supernatant before heating again to 95°C. Both nonreducing and reducing samples were resolved on 15% SDS-PAA gels and analyzed by phosphor imaging.

Western blot

B cells were activated with 20 $\mu\text{g}/\text{mL}$ LPS for up to 4 days. Cells were harvested by centrifugation, washed once with Dulbecco's phosphate buffered saline and subsequently lysed in RIPA buffer (50 mM Tris-HCl pH 8, 150 mM NaCl, 1% Igepal, 0.1% SDS, 0.5% deoxycholate) containing protease inhibitors (1 mM PMSF and 10 $\mu\text{g}/\text{mL}$ CLAP). Lysates were resolved on 15% SDS-PAA gels and transferred to polyvinylidene fluoride (PVDF). Specific rabbit polyclonal antibodies were used to probe for CNPY2, 3, 4, and 5. Mouse anti-Tubulin (Synaptic systems) was included as loading control. Goat-anti-mouse IRDye 800 CW (LI-Cor) and Donkey-

anti-Rabbit-Alexa Fluor 688 (Thermo Fisher) secondary antibodies were used and blots were visualized on an Odyssey[®] CLx imager.

Quantitative polymerase chain reaction

RNA was extracted using TRI Reagent (Sigma), and cDNA was synthesized by RevertAid Premium Reverse Transcriptase (Fermentas) using poly-dT primers. To detect CNPY mRNA changes during B-cell activation, B cells were cultured with 20 $\mu\text{g}/\text{mL}$ LPS for 4 days with samples taken each day. Cells were lysed in TRIzol, and mRNA was extracted with Direct-zol RNA miniprep kit (Zymogen). Real-time PCR (RT-PCR) reactions were performed on the Viia7[™] system (Thermo Fisher) using SYBR green PCR master mix. qPCR reaction efficiencies were analyzed and threshold cycle values were used to assess the relative expression levels normalized to actin using the $2(-\Delta\Delta\text{Ct})$ method. Data represent the mean of three biological replicates analyzed in triplicate \pm SEM.

XBP1 splicing

Resting and LPS-activated B cells were lysed in Trizol, and RNA was extracted (Direct-zol RNA miniprep kit, Zymogen). cDNA was synthesized using poly-dT oligos and recombinant M-MuLV RT (RevertAid First Strand cDNA Synthesis Kit, Thermo Fisher). Spliced and unspliced XBP1 cDNA were amplified by PCR with the following forward: ACACGCTTGGGAATGGACAC and reverse: CCATGGGAAGATGTTCTGGG primers. Amplicons were analyzed on a 2% agarose gel.

Other methods

Signal peptide predictions were done with SignalP4.0 (38). Alignment of mouse CNPY and other SAPLIP amino acid sequences was done using ClustalW, and sequence analysis was completed in Jalview. Helical wheels were made with <http://rzlab.ucr.edu/scripts/wheel/wheel.cgi>. Western blot images were processed using Image Studio 5.2 (LiCoR).

Acknowledgment

We thank Dr. Joseline Houwman and Marcel van Willigen for proofreading and preparing figures.

Conflict of Interest

The authors declare no conflict of interest.

REFERENCES

1. Bruhn H (2005) A short guided tour through functional and structural features of saposin-like proteins. *Biochem J* 389:249–257.
2. Hirate Y, Okamoto H (2006) Canopy1, a novel regulator of FGF signaling around the midbrain-hindbrain boundary in zebrafish. *Curr Biol* 16:421–427.
3. Matsui T, Thitamadee S, Murata T, Kakinuma H, Nabetani T, Hirabayashi Y, Hirate Y, Okamoto H, Bessho Y (2011) Canopy1, a positive feedback regulator

- of FGF signaling, controls progenitor cell clustering during Kupffer's vesicle organogenesis. *Proc Natl Acad Sci U S A* 108:9881–9886.
4. Uhlén M, Fagerberg L, Hallström BM, Lindskog C, Oksvold P, Mardinoglu A, Sivertsson Å, Kampf C, Sjöstedt E, Asplund A, Olsson I, Edlund K, Lundberg E, Navani S, Szigartyo CA-K, Odeberg J, Djureinovic D, Takanen JO, Hober S, Alm T, Edqvist P-H, Berling H, Tegel H, Mulder J, Rockberg J, Nilsson P, Schwenk JM, Hamsten M, von Feilitzen K, Forsberg M, Persson L, Johansson F, Zwahlen M, von Heijne G, Nielsen J, Pontén F (2015) Tissue-based map of the human proteome. *Science* 347:1260419.
 5. Bornhauser BC, Olsson PA, Lindholm D (2003) MSAP is a novel MIR-interacting protein that enhances neurite outgrowth and increases myosin regulatory light chain. *J Biol Chem* 278:35412–35420.
 6. Guo J, Zhang Y, Mihic A, Li S-H, Sun Z, Shao Z, Wu J, Weisel RD, Li R-K (2015) A secreted protein (Canopy 2, CNPY2) enhances angiogenesis and promotes smooth muscle cell migration and proliferation. *Cardiovasc Res* 105:383–393.
 7. Do HT, Tselykh TV, Mäkelä J, Ho TH, Olkkonen VM, Bornhauser BC, Korhonen L, Zelcer N, Lindholm D (2012) Fibroblast growth factor-21 (FGF21) regulates low-density lipoprotein receptor (LDLR) levels in cells via the E3-ubiquitin ligase Mylip/Idol and the Canopy2 (Cnp2)/Mylip-interacting saposin-like protein (Msap). *J Biol Chem* 287:12602–12611.
 8. Yan P, Gong H, Zhai X, Feng Y, Wu J, He S, Guo J, Wang X, Guo R, Xie J (2016) Decreasing CNPY2 expression diminishes colorectal tumor growth and development through activation of p53 pathway. *Am J Pathol* 186:1015–1024.
 9. Shimura M, Mizuma M, Takadate T, Katoh Y, Suzuki T, Iseki M, Hata T, Aoki S, Suzuki Y, Sakata N (2018) A novel liver metastasis-correlated protein of pancreatic neuroendocrine neoplasm (PanNEN) discovered by proteomic analysis. *Oncotarget* 9:24291.
 10. Taniguchi H, Ito S, Ueda T, Morioka Y, Kayukawa N, Ueno A, Nakagawa H, Fujihara A, Ushijima S, Kanazawa M (2017) CNPY2 promoted the proliferation of renal cell carcinoma cells and increased the expression of TP53. *Biochem Biophys Res Commun* 485:267–271.
 11. Wang D, Wang Z-M, Zhang S, Wu H-J, Tao Y-M (2018) Canopy homolog 2 expression predicts poor prognosis in hepatocellular carcinoma with tumor hemorrhage. *Cell Physiol Biochem* 50:2017–2028.
 12. Mutoh H, Kato M, Akita T, Shibata T, Wakamoto H, Ikeda H, Kitaura H, Aoto K, Nakashima M, Wang T (2018) Biallelic variants in CNPY3, encoding an endoplasmic reticulum chaperone, cause early-onset epileptic encephalopathy. *Am J Hum Genet* 102:321–329.
 13. Takahashi K, Shibata T, Akashi-Takamura S, Kiyokawa T, Wakabayashi Y, Tanimura N, Kobayashi T, Matsumoto F, Fukui R, Kouro T, Nagai Y, Takatsu K, Saitoh S-i, Miyake K (2007) A protein associated with toll-like receptor (TLR) 4 (PRAT4A) is required for TLR-dependent immune responses. *J Exp Med* 204:2963–2976.
 14. Liu B, Yang Y, Qiu Z, Staron M, Hong F, Li Y, Wu S, Li Y, Hao B, Bona R, Han D, Li Z (2010) Folding of toll-like receptors by the HSP90 paralogue gp96 requires a substrate-specific cochaperone. *Nat Commun* 1:79–79.
 15. Morales C, Li Z (2017) *Drosophila* canopy b is a cochaperone of glycoprotein 93. *J Biol Chem* 292:6657–6666.
 16. Faraz M, Herdenberg C, Holmlund C, Henriksson R, Hedman H (2018) A protein interaction network centered on leucine-rich repeats and immunoglobulin-like domains 1 (LRIG1) regulates growth factor receptors. *J Biol Chem* 293:3421–3435.
 17. Konno K, Wakabayashi Y, Akashi-Takamura S, Ishii T, Kobayashi M, Takahashi K, Kusumoto Y, Saitoh S-i, Yoshizawa Y, Miyake K (2006) A molecule that is associated with toll-like receptor 4 and regulates its cell surface expression. *Biochem Biophys Res Commun* 339:1076–1082.
 18. Wakabayashi Y, Kobayashi M, Akashi-Takamura S, Tanimura N, Konno K, Takahashi K, Ishii T, Mizutani T, Iba H, Kouro T, Takaki S, Takatsu K, Oda Y, Ishihama Y, Saitoh S-i, Miyake K (2006) A protein associated with toll-like receptor 4 (PRAT4A) regulates cell surface expression of TLR4. *J Immunol* 177:1772–1779.
 19. Shibata T, Takemura N, Motoi Y, Goto Y, Karuppuchamy T, Izawa K, Li X, Akashi-Takamura S, Tanimura N, Kunisawa J, Kiyono H, Akira S, Kitamura T, Kitaura J, Uematsu S, Miyake K (2012) PRAT4A-dependent expression of cell surface TLR5 on neutrophils, classical monocytes and dendritic cells. *Int Immunol* 24:613–623.
 20. Randow F, Seed B (2001) Endoplasmic reticulum chaperone gp96 is required for innate immunity but not cell viability. *Nat Cell Biol* 3:891–896.
 21. Hart BE, Tapping RI (2012) Cell surface trafficking of TLR1 is differentially regulated by the chaperones PRAT4A and PRAT4B. *J Biol Chem* 287:16550–16562.
 22. Van Anken E, Romijn EP, Maggioni C, Mezghrani A, Sitia R, Braakman I, Heck AJ (2003) Sequential waves of functionally related proteins are expressed when B cells prepare for antibody secretion. *Immunity* 18:243–253.
 23. Romijn EP, Christis C, Wiewer M, Gouw JW, Fullaondo A, van der Sluijs P, Braakman I, Heck AJ (2005) Expression clustering reveals detailed co-expression patterns of functionally related proteins during B cell differentiation: a proteomic study using a combination of one-dimensional gel electrophoresis, LC-MS/MS, and stable isotope labeling by amino acids in cell culture (SILAC). *Mol Cell Proteomics* 4:1297–1310.
 24. Shimizu Y, Meunier L, Hendershot LM (2009) pERp1 is significantly up-regulated during plasma cell differentiation and contributes to the oxidative folding of immunoglobulin. *Proc Natl Acad Sci U S A* 106:17013–17018.
 25. van Anken E, Pena F, Hafkemeijer N, Christis C, Romijn EP, Grauschopf U, Oorschot VMJ, Pertel T, Engels S, Ora A, Lástun V, Glockshuber R, Klumperman J, Heck AJR, Luban J, Braakman I (2009) Efficient IgM assembly and secretion require the plasma cell induced endoplasmic reticulum protein pERp1. *Proc Natl Acad Sci U S A* 106:17019–17024.
 26. Flach H, Rosenbaum M, Duchniewicz M, Kim S, Zhang SL, Cahalan MD, Mittler G, Grosschedl R (2010) Mzb1 protein regulates calcium homeostasis, antibody secretion, and integrin activation in innate-like B cells. *Immunity* 33:723–735.
 27. Rosenbaum M, Andreani V, Kapoor T, Herp S, Flach H, Duchniewicz M, Grosschedl R (2014) MZB1 is a GRP94 cochaperone that enables proper immunoglobulin heavy chain biosynthesis upon ER stress. *Genes Dev* 28:1165–1178.
 28. Anelli T, van Anken E (2013) Missing links in antibody assembly control. *Int J Cell Biol* 2013:9.
 29. Worah K, Mathan TS, Manh TPV, Keerthikumar S, Schreiber G, Tel J, Duiveman-de Boer T, Sköld AE, van Spriel AB, de Vries IJM (2016) Proteomics of human dendritic cell subsets reveals subset-specific surface markers and differential inflammasome function. *Cell Rep* 16:2953–2966.
 30. Meunier L, Usherwood Y-K, Chung KT, Hendershot LM (2002) A subset of chaperones and folding enzymes form multiprotein complexes in endoplasmic reticulum to bind nascent proteins. *Mol Biol Cell* 13:4456–4469.

31. Hong F, Mohammad Rachidi S, Lundgren D, Han D, Huang X, Zhao H, Kimura Y, Hirano H, Ohara O, Udono H, Meng S, Liu B, Li Z (2017) Mapping the interactome of a major mammalian endoplasmic reticulum heat shock protein 90. *PLoS One* 12:e0169260.
32. Liepinsh E, Andersson M, Ruysschaert J-M, Otting G (1997) Saposin fold revealed by the NMR structure of NK-lysin. *Nat Struct Biol* 4:793–795.
33. Wang C, Yu J, Wang L, Feng W, Wang C (2012) Human protein-disulfide isomerase is a redox-regulated chaperone activated by oxidation of domain a'. *J Biol Chem* 287:1139–1149.
34. Malinina L, Patel DJ, Brown RE (2017) How alpha-helical motifs form functionally diverse lipid-binding compartments. *Annu Rev Biochem* 86:609–636.
35. Mysliwy J, Dingley AJ, Stanisak M, Jung S, Lorenzen I, Roeder T, Leippe M, Grötzinger J (2010) Caenopore-5: the three-dimensional structure of an antimicrobial protein from *Caenorhabditis elegans*. *Dev Comp Immunol* 34:323–330.
36. Hill CH, Cook GM, Spratley SJ, Fawke S, Graham SC, Deane JE (2018) The mechanism of glycosphingolipid degradation revealed by a GALC-SapA complex structure. *Nat Commun* 9:151.
37. Xiong Z-J, Huang J, Poda G, Pomès R, Privé GG (2016) Structure of human acid sphingomyelinase reveals the role of the saposin domain in activating substrate hydrolysis. *J Mol Biol* 428:3026–3042.
38. Petersen TN, Brunak S, von Heijne G, Nielsen H (2011) SignalP 4.0: discriminating signal peptides from transmembrane regions. *Nat Methods* 8:785–786.
39. Raykhel I, Alanen H, Salo K, Jurvansuu J, Nguyen VD, Latva-Ranta M, Ruddock L (2007) A molecular specificity code for the three mammalian KDEL receptors. *J Cell Biol* 179:1193–1204.
40. Alanen HI, Raykhel IB, Luukas MJ, Salo KE, Ruddock LW (2011) Beyond KDEL: the role of positions 5 and 6 in determining ER localization. *J Mol Biol* 409:291–297.
41. Ellgaard L, Sevier CS, Bulleid NJ (2018) How are proteins reduced in the endoplasmic reticulum? *Trends Biochem Sci* 43:32–43.
42. Appenzeller-Herzog C, Ellgaard L (2008) In vivo reduction-oxidation state of protein disulfide isomerase: the two active sites independently occur in the reduced and oxidized forms. *Antioxid Redox Signal* 10:55–64.
43. Montero D, Tachibana C, Winther JR, Appenzeller-Herzog C (2013) Intracellular glutathione pools are heterogeneously concentrated. *Redox Biol* 1: 508–513.
44. O'Brien H, Kanemura S, Okumura M, Baskin RP, Bandyopadhyay PK, Olivera BM, Ellgaard L, Inaba K, Safavi-Hemami H (2018) Ero1-mediated reoxidation of protein disulfide isomerase accelerates the folding of cone snail toxins. *Int J Mol Sci* 19:3418.
45. Tatu U, Braakman I, Helenius A (1993) Membrane glycoprotein folding, oligomerization and intracellular transport: effects of dithiothreitol in living cells. *EMBO J* 12:2151–2157.
46. Gardner BM, Pincus D, Gotthardt K, Gallagher CM, Walter P (2013) Endoplasmic reticulum stress sensing in the unfolded protein response. *Cold Spring Harbor Perspect Biol* 5:a013169–a013169.
47. Scheuner D, Song B, McEwen E, Liu C, Laybutt R, Gillespie P, Saunders T, Bonner-Weir S, Kaufman RJ (2001) Translational control is required for the unfolded protein response and in vivo glucose homeostasis. *Mol Cell* 7:1165–1176.
48. Christis C, Fullaondo A, Schildknecht D, Mkrtchian S, Heck AJ, Braakman I (2010) Regulated increase in folding capacity prevents unfolded protein stress in the ER. *J Cell Sci* 123:787–794.
49. Sevier CS, Qu H, Heldman N, Gross E, Fass D, Kaiser CA (2007) Modulation of cellular disulfide-bond formation and the ER redox environment by feedback regulation of Ero1. *Cell* 129:333–344.
50. Weekes MP, Antrobus R, Talbot S, Hör S, Simecek N, Smith DL, Bloor S, Randow F, Lehner PJ (2012) Proteomic plasma membrane profiling reveals an essential role for gp96 in the cell surface expression of LDLR family members, including the LDL receptor and LRP6. *J Proteome Res* 11:1475–1484.
51. Sprong H, Kruithof B, Leijendekker R, Slot JW, van Meer G, van der Sluijs P (1998) UDP-galactose:ceramide galactosyltransferase is a class I integral membrane protein of the endoplasmic reticulum. *J Biol Chem* 273: 25880–25888.
52. McCaul N, Yeoh HY, van Zadelhoff G, Lodder N, Kleizen B, Braakman I (2019) Analysis of protein folding, transport, and degradation in living cells by radioactive pulse chase. *JoVE* 144:e58952.